

Elastic scattering angular distribution in $^{10}\text{B} + ^{232}\text{Th}$ reaction

Shradha Dubey^{1,2}, D.C.Biswas¹, S. Mukherjee², D. Patel², Y.K. Gupta¹, G. Prajapati¹, B. N. Joshi¹, L.S. Danu¹, S.Mukhopadhyay¹, B.V. John¹, B.K. Nayak¹

¹Nuclear Physics Division, Bhabha Atomic Research Centre, Mumbai – 400085, India.

²Physics Department, Faculty of Science, M. S. University of Baroda, Vadodara-390002, India.

email: dcbiswas@barc.gov.in

Introduction:

Precise measurements of the elastic scattering angular distributions determine parameters of the real and imaginary parts of the nuclear interaction potential. From systematic analysis of elastic-scattering data involving tightly bound nuclei, the “threshold anomaly” (TA) has been observed in a number of systems [1]. One of the manifestations of this feature is a strong energy dependence of the optical model potential deduced from analyses of elastic scattering angular distributions at energies around the Coulomb barrier. This behaviour can be understood using a dispersion relation between the real and the imaginary parts of the optical potential [2]. In case of scattering with loosely bound projectiles, a different type energy dependence from that of TA is observed, which has been known as ‘breakup threshold anomaly’ (BTA) [3,4]. In this case, a repulsive real dynamical potential is generated by the coupling of breakup channels to the elastic scattering. For heavy targets, due to the large Coulomb effects the TA/BTA is expected to be more pronounced. Further measurements involving heavy targets with various projectiles are required to understand the systematics of TA and BTA.

In the present work, the results on investigation of elastic scattering for $^{10}\text{B} + ^{232}\text{Th}$ system have been reported through very precise and complete angular distribution measurements at energies from below to above the Coulomb barrier. The total reaction cross sections for this system have also been derived in order to investigate the role of breakup on the total reaction cross section.

Experimental details:

The experiment was performed using ^{10}B beam from BARC-TIFR Pelletron facility,

Mumbai, India. The beam was bombarded on self supporting ^{232}Th target of thickness 1.5 mg/cm^2 and the elastically scattered ^{10}B ion were detected by four silicon surface barrier detectors in ΔE -E telescopic arrangements. The telescopes used had a thickness (T_1) with $\Delta E = 25 \mu\text{m}$ and $E = 300 \mu\text{m}$, (T_2) with $\Delta E = 40 \mu\text{m}$ and $E = 300 \mu\text{m}$, (T_3) with $\Delta E = 25 \mu\text{m}$ and $E = 300 \mu\text{m}$ and (T_4) with $\Delta E = 25 \mu\text{m}$ and $E = 300 \mu\text{m}$. Two monitor detectors with thickness around $300 \mu\text{m}$ were used for absolute normalization and beam monitoring. The measurements were carried out for different beam energies covering a wide range from 49 to 65 MeV.

Results and discussion:

The elastic scattering angular distribution measurements have been carried out in a wide angular range from 35° to 170° . The ratios of elastic to the Rutherford scattering cross sections have been plotted as a function of scattering angle ($\theta_{\text{c.m.}}$) for various bombarding energies as shown in Fig.1. The optical model analysis of the elastic scattering data were performed using the ECIS code [5]. In the fitting procedure the real and imaginary diffuseness parameters (a_r and a_w) were kept fixed and only the strength of real and imaginary potential parameters (V_r and V_i) were varied to obtain the best-fit of the experimental data. Overall very good fits to the experimental data were obtained at all energies as shown in Fig.1. The relevant parameters that provide a best fit to the elastic scattering angular distribution were obtained through a χ^2 -minimization procedure.

The corresponding energy dependence of the potential parameters are also shown in Fig. 2. It can be seen that in (Fig.2) the real potential parameters increases and the imaginary potential parameters decreases as the bombarding energy decreases towards the Coulomb barrier. This behaviour is the

indication of the usual threshold anomaly in $^{10}\text{B} + ^{232}\text{Th}$ system from the energy dependence of the potential parameters.

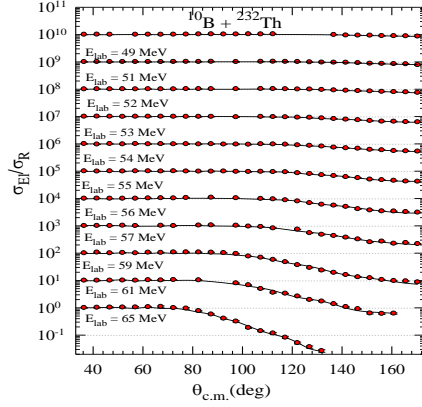


Fig.1: Elastic scattering angular distribution for the $^{10}\text{B} + ^{232}\text{Th}$ system at different beam energies. The solid lines are optical–model fits to the data using the ECIS code.

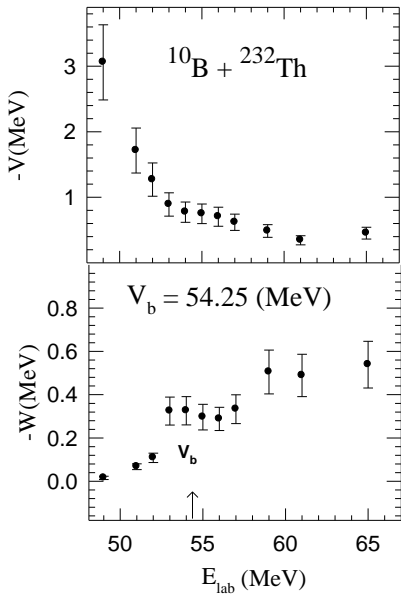


Fig. 2: Energy dependence of the real and imaginary part of the potential obtained for the $^{10}\text{B} + ^{232}\text{Th}$ system at a sensitive radius $R_s = 12.14 \text{ fm}$.

The total reaction cross-section obtained from the fitting of the elastic scattering data has been plotted in Fig.3. The fusion cross section values obtained by using

CCFULL code [6] and also the earlier measured fission cross section data taken from literature [7] are plotted in Fig. 3. At energies near the Coulomb barrier, it is observed that the total reaction cross section is significantly large in comparison to the fission cross section as well as fusion cross section of $^{10}\text{B} + ^{232}\text{Th}$ system as shown in Fig. 3. This can be explained due to the lower breakup threshold energy for the ^{10}B (4.46 MeV). More detailed analysis with different form of the potential is being carried out and the results will be presented in the symposium.

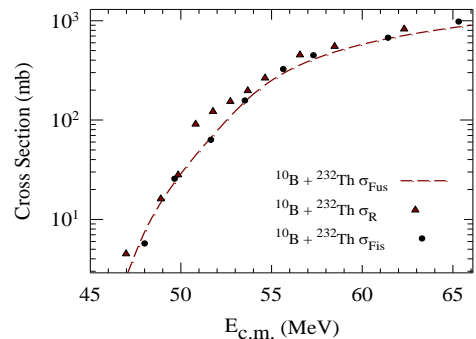


Fig.3: Total fusion cross sections (σ_{Fus}), total reaction cross sections (σ_{R}) and total fission cross sections (σ_{Fis}) for $^{10}\text{B} + ^{232}\text{Th}$ system as a function of the bombarding energies.

Acknowledgments:

We are thankful to BARC-TIFR pelletron staff for smooth running of the machine during experiment. This work is partially supported by a research project being financed by UGC-DAE-CSR, Kolkata.

References:

1. G.R. Satchler, Phys. Rep. **199**, 147(1991).
2. A. Shrivastava et al., Nucl. A **635**, 411 (1998).
3. N. N. Deshmukh et al., Phys. Rev. C **83**, 024607 (2011).
4. Shradha Dubey et al., Phys. Rev. C **89**, 014610 (2014).
5. J. Raynal, Phys. Rev. C **23**, 2571 (1981).
6. K. Hagino et al., comput. Phys. **123**, 143 (1999).
7. B. K. Nayak et al., Phys. Rev. C **62**, 031601 (2000).